Available online at www.sciencedirect.com
ScienceDirect
Bioorganic & Medicinal Chemistry 15 (2007) 7840–7849
Bioorganic & Medicinal Chemistry

Photomodulation of PS-modified oligonucleotides containing azobenzene substituent at pre-selected positions in phosphate backbone

Satyakam Patnaik,[a] P. Kumar,[a] B. S. Garg,[b] R. P. Gandhi[c] and K. C. Gupta[a,*]

[a]*Nucleic Acids Research Laboratory, Institute of Genomics and Integrative Biology, Mall Road, Delhi University Campus, Delhi 110 007, India*
[b]*Department of Chemistry, University of Delhi, Delhi 110 007, India*
[c]*Dr. B.R. Ambedkar Center for Biomedical Research, University of Delhi, Delhi 110 007, India*

Received 27 April 2007; revised 21 August 2007; accepted 23 August 2007
Available online 28 August 2007

Abstract—A new protocol has been developed for incorporation of a photoisomerizable azobenzene moiety into synthetic stereo-enriched [R_p] and [S_p] PS-oligonucleotides. The azobenzene pendant is attached at pre-selected positions in internucleotidic phosphorothioate oligonucleotides of both [R_p] and [S_p] diastereomers using a novel reagent, *N*-iodoacetyl-*p*-aminoazobenzene, **1**. The modified oligomers are purified on HPLC, characterized by LC–MS, and examined for their thermal and photoisomerization properties. The azobenzene moiety imparts greater stability to oligomer duplexes in (*E*) N=N configuration as compared to (*Z*) configuration. The placement of the azobenzene pendant close to 5′-terminus ($n - 1$) and 3′-terminus of the modified PS-oligos contributes maximum stability to the duplex while a gradual decline in stability occurs with azobenzene moving toward middle of the duplex. Circular Dichroism studies reveal that the chiral environment at the phosphorus center of the PS-oligos does not alter the global conformation of the DNA duplex as such, suggesting conservation of conformation of the modified DNA strands.
© 2007 Elsevier Ltd. All rights reserved.

1. Introduction

Recently, much attention has been focused on artificial control of bio-chemical reactions.[1] The most cited example of this phenomenon is the regulation of gene expression, which can be achieved by addition of a short oligonucleotide (12–15 mer) either at transcriptional (antigene) or translational (antisense) stage. An alternative methodology is based on the use of isomerizable structural moieties where regulation is controlled by external means, i.e., light. Literature records sporadic studies[1–3] relating to control of enzyme activity, receptor binding properties, membrane permeability, electron transfer, peptide conformation, etc., where macroscopic properties of biomolecules have been altered using UV–vis radiation. Although, a number of photoisomerizable groups have been developed, azobenzene molecule has attracted considerable attention because of ease of its preparation and efficient photoisomerization property (*E*–*Z* transformation).[2–5] Yamana et al. have successfully incorporated azobenzene moiety as a bridge between two oligo strands via the 5′-end of one oligo and the 3′-end of the other.[6] They further report incorporation of phosphoramidite reagents of various derivatives of azobenzene having different substituents at *p*-, *p*′-positions of the two phenyl rings for linking two oligo strands[7] and have examined photomodulation of some duplex structures. In a series of papers, Komiyama et al.[8–18] have reported on photoregulation of enzyme activity of T7 RNA polymerase by tethering an azobenzene to the promoter and regulating the activity of T7 DNA polymerase by photoresponsive oligonucleotide as modulator,[10,11] and have further studied triplex formation and dissociation by tethering azobenzene to the third strand of the triplex.[12–14] Their approach entails the use of phosphoramidite reagent based on azobenzene-linked 2,2-bis (hydroxymethyl)-propionic acid for subsequent incorporation into oligonucleotides at various positions during synthesis. In the above studies, the *E*-isomer has been demonstrated to be more

Keywords: PS-oligomers; Azobenzene; *E*–*Z* photoisomerization; Hybridization; Circular Dichroism.
* Corresponding author. Tel.: +91 11 27662491; fax: +91 11 27667471; e-mail: kcgupta@igib.res.in

0968-0896/$ - see front matter © 2007 Elsevier Ltd. All rights reserved.
doi:10.1016/j.bmc.2007.08.042

stable than the corresponding *Z*-isomer in both [R_p] and [S_p] diastereomers. In another approach, Komiyama et al.[9] have tethered an azobenzene pendant at 2′-position of uridine followed by its incorporation into oligonucleotides using phosphoramidite approach. However, a differential stability behavior has been reported for the synthetic photoresponsive oligonucleotide containing *m*-aminoazobenzene substituent.[18]

In this communication, we report a new convenient protocol for tethering an azobenzene moiety to synthetic PS-oligos at pre-selected positions in the backbone. This method is based on the use of a novel reagent, *N*-iodoacetyl-*p*-aminoazobenzene, **1**, which is attached to purified diastereomers [R_p] and [S_p] of phosphorothioate oligonucleotides. The paper also records a detailed study of stability characteristics of duplexes of modified PS-oligonucleotides and unmodified complementary oligonucleotides as a function of the position of the azobenzene (which moves from 3′-end toward the 5′-end of the duplex), both under experimental conditions (Δ) as well as under photoirradiations (h*ν*).

2. Results and discussion

In designing a facile methodology for incorporation of azobenzene moiety into the oligonucleotide chains, we preferred incorporation of PS-linkage in the oligomer sequence at pre-selected positions based on the knowledge that iodo-alkyl reagents are specific toward PS-linkages. This synthetic protocol eliminates the steps associated with the phosphoramidite monomer (used by the Komiyama's group) and reduces the formation of intermediates in the synthetic sequence. The synthesis of the reagent, *N*-iodoacetyl-*p*-aminoazobenzene, **1**, was accomplished through coupling of *p*-aminoazobenzene with iodoacetic acid in the presence of dicyclohexylcarbodiimide in 80% yield (Scheme 1). This was characterized through IR, ^{1}H NMR, ES-MS mass spectrometry, and elemental analysis.

2.1. Modified oligonucleotides: synthesis and purification

PS-oligonucleotides (Table 1) were synthesized on normal and modified supports (**A**, Scheme 2) on a Pharmacia Gene Assembler Plus using the phosphoramidite approach. The phosphorothioate linkages (PS) were introduced in the machine itself at desired sites using tetraethylthiuram disulfide (TETD) in place of a conventional oxidation reagent. The cleavage of modified PS-oligonucleotides from the solid support and removal of protecting groups from the backbone and nucleobases were achieved in a single step by treatment with aqueous NH_4OH (30%, 55 °C, 16 h). The purification and characterization of each of the diasteromers of oligonucleotides were done as described in Section 4. The elution pattern shows that [R_p] isomer has less retention time as compared to its [S_p] counterpart which elutes later having a higher retention time[19,20] (Fig. 1a and b).

2.2. Covalent attachment of azobenzene pendant to PS-oligonucleotides

The covalent attachment of the azobenzene pendant to the PS-oligonucleotides was achieved by treating the PS-oligonucleotides with an excess of **1** (Scheme 3). The purification and characterization were done vide experimental to yield the oligonucleotide conjugates in almost quantitative yield. Figure 1a and b shows HPLC profiles of [R_p] and [S_p] diastereomers of PS-4 phosphorothioate oligonucleotide while, Figure 1c and d depicts a co-injection of [R_p] and [S_p] diastereomers of PS-4 oligomer and azobenzene linked [R_p] diastereomer of PS-4 oligonucleotide, respectively.

Similarly, other conjugates were prepared, purified, and analyzed.

2.3. Photomodulation of single stranded oligonucleotides containing azobenzene moiety

The azobenzene-tethered modified oligonucleotides exhibit two distinct absorption bands at ~343 and ~434 nm along with the characteristic band at around 260 nm, which has not been shown for the sake of clarity. The former band is attributed to π–π^* transition in azobenzene and, under normal conditions, all phosphorothioate oligomers with azobenzene residue predominantly comprise of the thermodynamically stable *E*-isomer. Figure 2 (top) shows UV and (bottom) HPLC profiles of purified [S_p] diastereomer of PS-1. It was observed that, on irradiating (365 nm) PS-1 [S_p] diastereomer over a period of time (curve a, top), the intensity of the band at ~343 nm (*E*-isomer, 91.6%) decreased with concurrent increase in intensity of band at ~434 nm, *Z*-isomer (curve b, top). The photostationary state was obtained within 30 min of irradiation (365 nm) (17.7% of *Z*-isomer), which reflects no further increment in the band intensity at ~434 nm. When the above sample was further exposed to visible light ($\lambda > 400$ nm), the peak corresponding to *Z*-isomer of the PS-1 [S_p] diastereomer displayed a decrease in intensity (with corresponding increase in the peak at 343 nm due to the *E*-isomer, i.e., 89%) [curve c]. HPLC profiles (bottom) also corroborate the above photoreversibility effect. Profile (a), Figure 2 (bottom) shows the elution pattern of PS-1 ([S_p] diastereomer) prior to irradiation

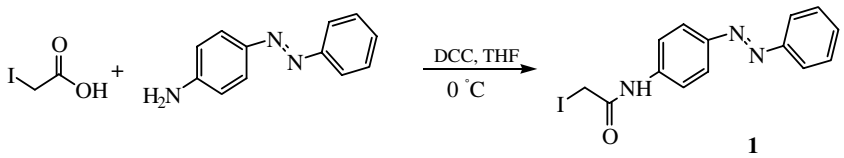

Scheme 1. Preparation of azobenzene pendant **1**.

Table 1. Oligonucleotide sequences[a]

Oligomers	Diastereomeric mixed sequences	Observed mass (M + Na^+)	Internucleotide linkage
PO-1	d(TTTTTTTT)	2394	Phosphate
PO-2	d(AAAAAAAA)	2474	Phosphate
PS-1	d(TTTTTTT_{ps}T) [R_p/S_p]	2410	Phosphorothioate
PS-2	d(TTTTTT_{ps}TT) [R_p/S_p]	2410	Phosphorothioate
PS-3	d(TTTTT_{ps}TTT) [R_p/S_p]	2410	Phosphorothioate
PS-4	d(TTTT_{ps}TTTT) [R_p/S_p]	2410	Phosphorothioate
PS-5	d(TTT_{ps}TTTTT) [R_p/S_p]	2410	Phosphorothioate
PS-6	d(TT_{ps}TTTTTT) [R_p/S_p]	2410	Phosphorothioate
PS-7	d(T_{ps}TTTTTTT) [R_p/S_p]	2410	Phosphorothioate
PS-8[b]	d(TTTTTTTT_{ps})	2473	Thiophosphate
PS-9	d(AAAAAAA_{ps}A) [R_p/S_p]	2490	Phosphorothioate
PS-10	d(AAAAAA_{ps}AA) [R_p/S_p]	2490	Phosphorothioate
PS-11	d(AAAAA_{ps}AAA) [R_p/S_p]	2490	Phosphorothioate
PS-12	d(AAAA_{ps}AAAA) [R_p/S_p]	2490	Phosphorothioate
PS-13	d(AAA_{ps}AAAAA) [R_p/S_p]	2490	Phosphorothioate
PS-14	d(AA_{ps}AAAAAA) [R_p/S_p]	2490	Phosphorothioate
PS-15	d(A_{ps}AAAAAAA) [R_p/S_p]	2490	Phosphorothioate
PS-16[b]	d(AAAAAAAA_{ps})	2553	Thiophosphate

[a] **ps** denotes position of the phosphorothioate/thiophosphate linkage in T-modified and A-modified strands.
[b] These oligonucleotides do not have diastereomers.

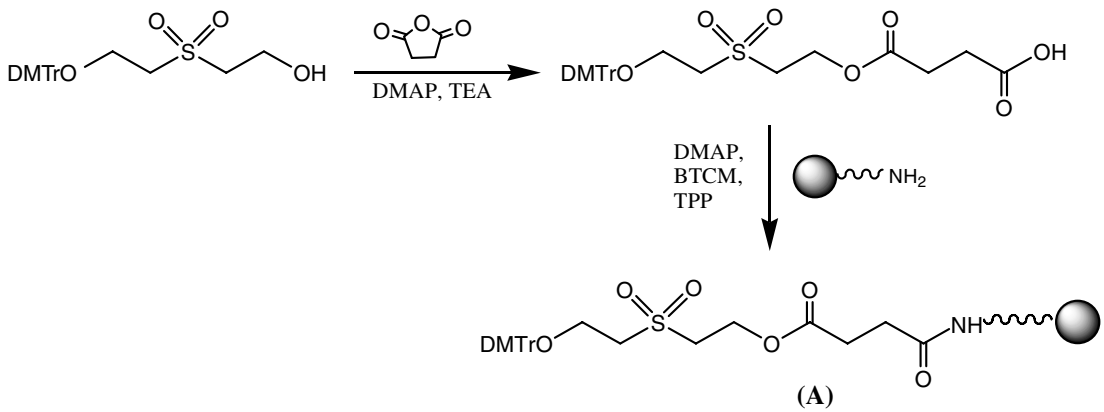

Scheme 2. Preparation of polymer support (**A**) for synthesis of thiophosphorylated oligonucleotides.

while profile (b) depicts the pattern when PS-1 [S_p] diastereomer is irradiated (365 nm). Photoreversible *E–Z* isomerization is depicted in profile (c) when the above sample was again exposed to visible radiation ($\lambda > 400$ nm). The above observations also lend credence to the fact that azobenzene moiety is tethered to the PS-modified oligonucleotides.

2.4. Photomodulation of duplexes containing azobenzene moiety

The T_m values for duplexes of a series of PS-modified homothymidines [$\mathbf{T_ppsT_q}$] and homoadenosines [$A_x$psA$_y$] with their corresponding complementary strands are given in Table 2, while Table 3 incorporates T_m data on azobenzene-tethered phosphorothioate modified homothymidines [$\mathbf{T_pXT}_q$] and homoadenosines [A_xXA_y]. Of particular significance is the difference in T_m values for [R_p] and [S_p] isomers (Table 2). Such differential stability characteristics of [R_p] and [S_p] isomers have been attributed to the difference in conformational adjustments caused by inward-oriented [R_p] vs outward-oriented [S_p] PS-moiety in the B-helix of the diastereomeric analogues of DNA.[21,22]

The T_m of native A_8/T_8 was found to be 22.3 °C. The T_m of the PS-modified duplex, $\mathbf{T_7XT/A_8}$ ([R_p] isomer), was observed at 35.2 °C (+12.9° and +9.8 °C with respect to T_m of A_8/T_8 and $\mathbf{T_7psT/A_8}$, respectively). When the same duplex was irradiated at 365 nm, the T_m changed to 28.2 °C (−7.0 °C with respect to *E*-isomer and +5.9 °C with respect to A_8/T_8 duplex). This substantial difference in the T_m value suggests that, in *E*-configuration, azobenzene, as a dangling aromatic residue, supposedly intercalates between the base pairs of the two complementary strands of the duplex, thereby enhancing stability of the duplex, whereas the duplex destabilizes with N=N attaining *Z*-configuration. This enhanced stability imparted by the azobenzene pendant, in *E*-configuration, may be related to preponderance of planar conformation of the *E*-isomer[23] that facilitates better base stacking effect as compared to the *Z*-isomer. The observation further suggests that the azobenzene moiety, in its *E*-configuration, effectively intercalates

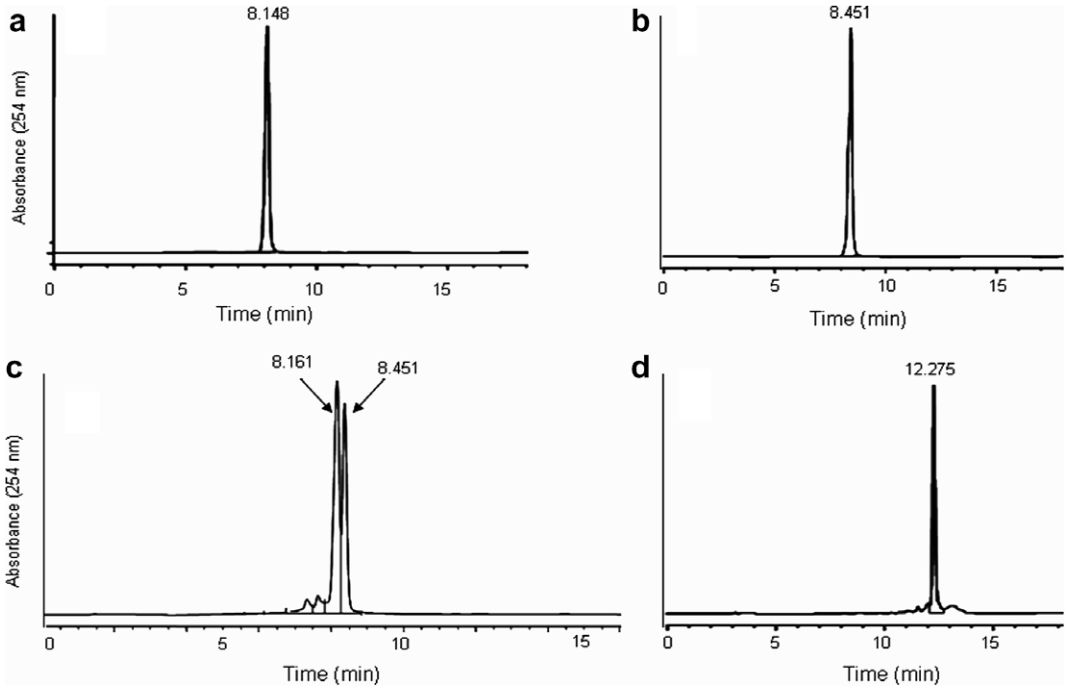

Figure 1. HPLC profiles of PS-4 phosphorothioate oligomer (a) [R_p] diastereomer, R_t = 8.148; (b) [S_p] diastereomer, R_t 8.451; (c) a co-injection of (a) and (b); (d) Azobenzene linked [R_p] diastereomer, R_t = 12.275. Conditions: Column, RP-18 Hypersil Gold; Gradient, 0–20% B in 15 min, A = 0.1 M $HCOONH_4$ buffer, pH 7.1, B = MeCN; flow rate, 1.0 ml/min.

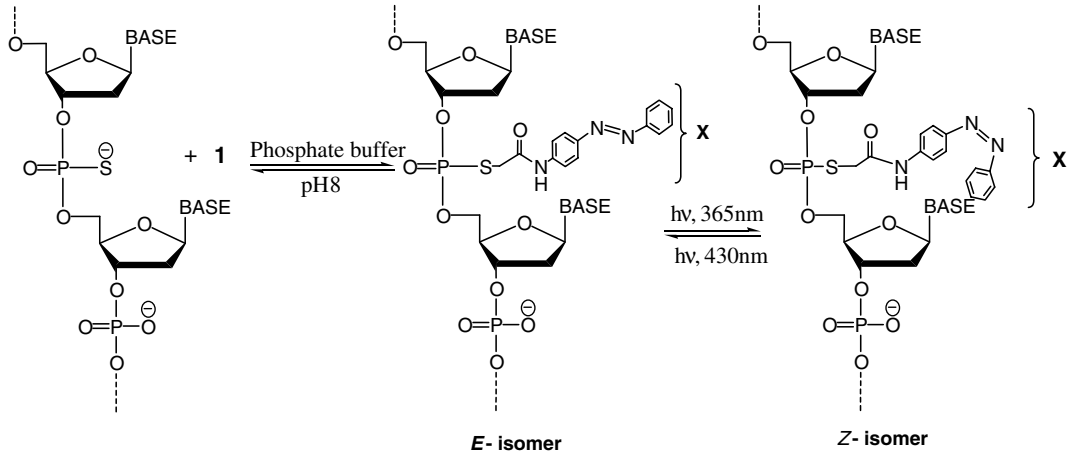

Scheme 3. Incorporation of azobenzene pendant **1** into synthetic oligonucleotides and photomodulation of azobenzene linked oligonucleotides under UV–vis light.

between the neighboring base pairs of the oligonucleotide duplex, while, in *Z*-configuration, it creates spatial distortion in the nearest base pairs, resulting in a destabilization of the duplex as compared to the *E*-configuration.[24–26] In case of PS-modified duplex, A_7XA/T_8 ([R_p] isomer), the same trend was observed although to a lesser extent where the *E*-isomer has a T_m of 28.3 °C (+6.0° and +5.1 °C with respect to A_8/T_8 and A_7psA/T_8, respectively) as against its *Z*-isomer which has a T_m of 23.3 °C (−5.0 °C with respect to *E*-isomer and +1.0 °C with respect to A_8/T_8). When the azobenzene moiety moves toward the middle of the modified strand, the stability of duplexes registers further decrease as evident in $\mathbf{T_5XT_3/A_8}$ ([R_p] isomer) where the T_m value of the *E*-isomer was observed to be 28.3 °C (+6.0 °C with respect to A_8/T_8), while in case of *Z*-isomer, the T_m value of 23.1 °C (−5.2 °C with respect to *E*-isomer and +0.8 °C with respect to A_8/T_8) was recorded due to a decrease in duplex stability.

Interestingly, with azobenzene placed in the middle of the duplex, in $\mathbf{T_4XT_4/A_8}$ ([R_p] isomer), the T_m value of the *E*-isomer was found to be 26.8 °C (+4.5° and +1.6 °C with respect to A_8/T_8 and $\mathbf{T_4psT_4/A_8}$, respectively), whereas a small decrease in stability results in case of *Z*-isomer, with T_m value of 22.8 °C (−4.0 °C with respect to *E*-isomer and +0.5 °C with respect to A_8/T_8). Likewise, when the azobenzene pendant is

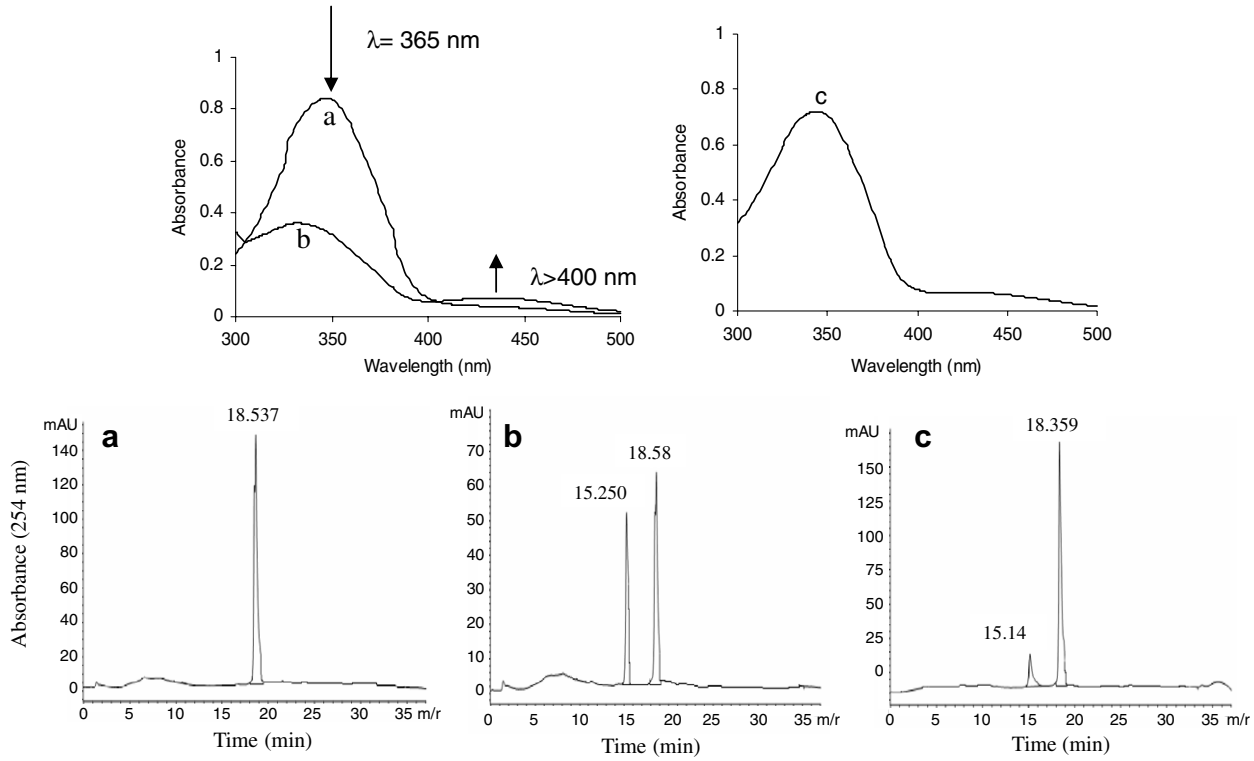

Figure 2. UV absorption patterns (top) and HPLC profiles (bottom) of PS-1 phosphorothioate oligo-([S_p] diastereomer), (a) before, and (b) after irradiation at λ = 365 nm. (c) Depicts spectral pattern when (b) is exposed to visible light (λ > 400 nm). Irradiation was carried out for 1 h at 303 K. Conditions: Column, RP-18 Hypersil Gold; Gradient, 0–15% B in 25 min, A = 0.1 M $HCOONH_4$ buffer, pH 7.1, B = MeCN; flow rate, 1.0 ml/min.

Table 2. Melting temperature (T_m) of duplexes between stereo-enriched oligos {[R_p] and [S_p]}, and their corresponding complementary sequences[a]

Duplex	T_m (°C)			
	[R_p] isomer	ΔT_m (ΔT_m w.r.t. native)	[S_p] isomer	ΔT_m (ΔT_m w.r.t. native)
A_7psA/T_8	23.2	(+0.9)	23.8	(+1.5)
A_4psA$_4$/T_8	23.3	(+1.0)	23.5	(+1.2)
T_7psT/A_8	25.4	(+3.1)	25.7	(+3.4)
T_4psT$_4$/A_8	25.2	(+2.9)	25.8	(+3.5)

[$A_x$psA$_y$] = [**$T_p$psT$_q$**] = [A_8] = [T_8] = 2 μM, 10 mM phosphate buffer containing 1.0 M NaCl, pH 7.1. **ps** denotes position of the phosphorothioate linkage in T-modified and A-modified strands.

[a] Values in Table 2 are average values of two observations per each oligo sequence. The reproducibility of T_m values was within [T_m ± 0.5 °C].

moved from the middle of the duplex towards the 5′-end, stability of the duplex shows an increase in the T_m value. This trend is observed in both the homopurine and homopyrimidine modified duplexes. Thus, in **T_2XT$_6$/A_8** ([R_p] isomer), the T_m value of the *E*-isomer was found to be 31.0 °C (+8.7 °C with respect to A_8/T_8), while that of its *Z*-isomer, the observed T_m value was 25.2 °C (−5.8 °C with respect to *E*-isomer and +2.9 °C with respect to A_8/T_8). Subsequently, in the case of AXA_7/T_8 ([R_p] isomer) duplex, the *E*-isomer had a T_m of 27.8 °C (+5.5 °C with respect to A_8/T_8) while, the stability of the above duplex, decreases (upon irradiation), with its passage into *Z*-isomer, that is, T_m of 22.9 °C (−4.9 °C with respect to *E*-isomer and +0.6 °C with respect to A_8/T_8). Figure 3a shows a typical thermal melting profile of the modified duplex A_3XA_5/T_8 ([S_p] isomer) before and after photoisomerization. In the above examples, the *E*–*Z* transformation of the azobenzene pendant (with attendant change in spectral characteristics) appeared reversible indicating that the azobenzene moiety is acting as a photomodulator of the oligomer duplexes. The *E*–*Z* isomerization is further supported by the observation that when the *Z*-isomer of A_3XA_5/T_8 ([S_p] isomer) was illuminated under visible light (λ > 400 nm) its melting profile almost superimposed with that of its *E*-counterpart (Fig. 3b).

In the modified duplex, **T_8X/A_8**, both in *E*- as well as *Z*-configurations, no significant change in stability occurred [+0.8 °C (*E*) to −0.9 °C (*Z*)] with respect to A_8/T_8, perhaps because of weak intra-strand stacking effect through the homopyrimidine strand.[27] However, in case of modified duplex, A_8X/T_8, the dangling azobenzene moiety does seem to impart a degree of stability [+1.8 °C (*E*) to −0.1 °C (*Z*)] to it.

From the data presented in Table 3, we conclude that in both the [R_p] and [S_p] isomeric series, the trans isomer enhances the stabilization of the duplexes with respect to the corresponding cis isomer; the azobenzene pendant, placed closed to 3′- and 5′-termini, confers maximum stability to the above duplexes, which registers a fall as the azobenzene pendant is moved towards the middle of the duplex. However, in all the above observa-

Table 3. Melting temperature (T_m) of duplexes between stereo-enriched oligos {[R_p] and [S_p]}, and their corresponding complementary sequences[a]

Duplex A_8/T_8 (native)	T_m (°C) = 22.3					
	[R_p] isomer			[S_p] isomer		
	E (ΔT_m w.r.t. native)	*Z* (ΔT_m w.r.t. native)	ΔT_m (*E*–*Z*)	*E* (ΔT_m w.r.t. native)	*Z* (ΔT_m w.r.t. native)	ΔT_m (*E*–*Z*)
A_7XA/T_8	28.3 (+6.0)	23.3 (+1.0)	5.0	26.9 (+4.6)	23.8 (+1.5)	3.1
A_6XA_2/T_8	24.1 (+1.8)	18.6 (−3.7)	5.5	23.6 (+1.3)	19.8 (−2.5)	3.8
A_5XA_3/T_8	20.6 (−1.7)	16.8 (−5.5)	3.8	17.7 (−4.6)	15.4 (−6.9)	2.3
A_4XA_4/T_8	18.4 (−3.9)	15.7 (−6.6)	2.7	16.3 (−6.0)	14.6 (−7.7)	1.7
A_3XA_5/T_8	21.0 (−1.3)	17.1 (−5.2)	3.9	17.9 (−4.4)	16.0 (−6.3)	1.9
A_2XA_6/T_8	24.5 (+2.2)	19.2 (−3.1)	5.3	23.2 (+0.9)	19.0 (−3.3)	4.2
AXA_7/T_8	27.8 (+5.5)	22.9 (+0.6)	4.9	27.1 (+4.8)	23.4 (+1.1)	3.7
A_8X/T_8[b]	24.1 (+1.8)	22.2 (−0.1)	1.9	—	—	—
T_7XT/A_8	35.2 (+12.9)	28.2 (+5.9)	7.0	29.5 (+7.2)	24.5 (+2.2)	5.0
T_6XT_2/A_8	31.6 (+9.3)	25.9 (+3.6)	5.7	26.2 (+3.9)	22.4 (+0.1)	3.8
T_5XT_3/A_8	28.3 (+6.0)	23.1 (+0.8)	5.2	24.9 (+2.6)	21.6 (−0.7)	3.3
T_4XT_4/A_8	26.8 (+4.5)	22.8 (+0.5)	4.0	23.1 (+0.8)	19.6 (−2.7)	3.5
T_3XT_5/A_8	27.9 (+5.6)	23.0 (+0.7)	4.9	24.2 (+1.9)	21.8 (−0.5)	2.4
T_2XT_6/A_8	31.0 (+8.7)	25.2 (+2.9)	5.8	26.0 (+3.7)	23.1 (+0.8)	2.9
TXT_7/A_8	33.4 (+11.1)	27.2 (+4.9)	6.2	27.9 (+5.6)	23.0 (+0.7)	4.9
T_8X/A_8[b]	23.1 (+0.8)	21.4 (−0.9)	1.7	—	—	—

[A_xXA_y] = [$\mathbf{T_pXT_q}$] = [A_8] = [T_8] = 2 μM, 10 mM phosphate buffer containing 1.0 M NaCl, pH 7.1. **X** = *N*-acetyl-*p*-aminoazobenzene linked to phosphorothioate backbone. [R_p] and [S_p] represent diastereomers of PS-oligos.

[a] Values in Table 3 are average values of two observations per each oligo sequence. The reproducibility of T_m values was within [T_m ± 0.5 °C]. The values in parentheses indicate ΔT_m of each of the entries with respect to T_m of the native.

[b] These entries do not have diastereomers.

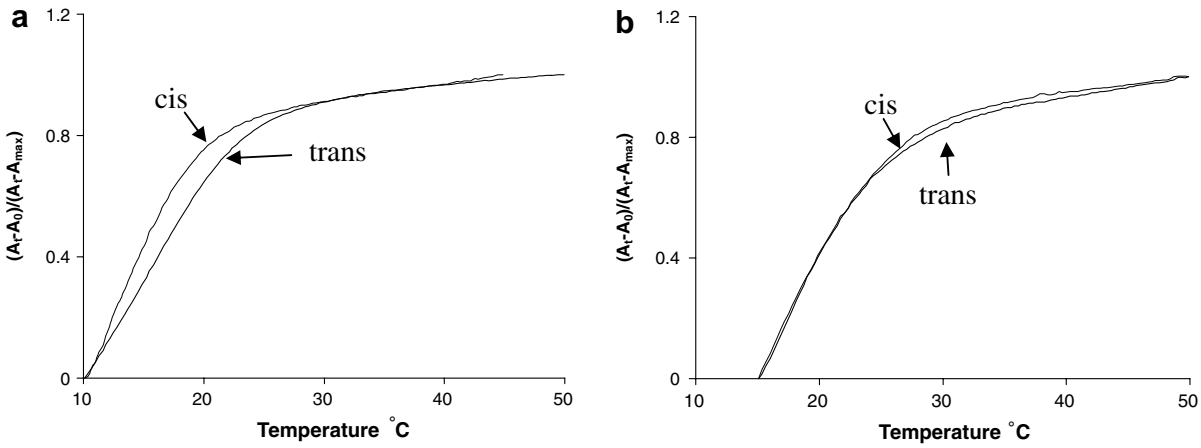

Figure 3. Thermal melting profile of (a) duplex A_3XA_5/T_8 ([S_p] isomer) before and after photoisomerization, (b) duplex A_3XA_5/T_8 ([S_p] isomer) (—) when exposed to UV irradiation (365 nm) and (----) when exposed to visible light (>400 nm).

tions the [R_p] isomers record greater stabilization as compared to the corresponding [S_p] isomers.

2.5. Circular Dichroism studies

It is well established that binding of an achiral ligand with DNA induces optical activity which is registered in induced Circular Dichroism (ICD) in the long-wavelength range of absorption of complex.[27] The binding of such a ligand or adduct along the helix axis of B-DNA induces ICD of two different categories: (i) groove-localized chromophores show strong positive ICD from transition moments oriented along the groove, and (ii) intercalated chromophores may display weaker positive or negative ICD.[28,29] To determine spatial orientation of the azobenzene moiety in the conjugated duplexes in the present investigation, the CD spectra were recorded at 10 °C ensuring complete association of the PS-modified oligo strand with its corresponding complementary strand. The normalized CD spectra of the PS-modified duplexes, after buffer subtraction, are shown in Figure 4. The CD spectrum of the unmodified duplex was similar to that of the native DNA having positive and negative CD bands of moderate magnitudes at wavelengths above 220 nm and a crossover point at ~242 nm. In addition, the PS-modified oligonucleotides exhibited weak CD (positive as well as negative) bands in the 300–400 nm region. The apparent difference of CD signatures, in this region, is perhaps due to increased flexibility in the phosphorothioate modified oligonucleotide strand.

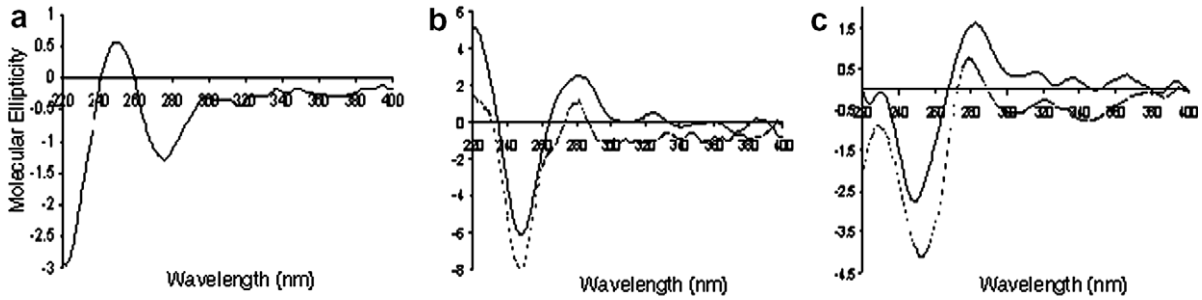

Figure 4. CD spectra of (a) native duplex (A_8/T_8), (b) [R_p]-A_5XA_3/T_8, (c) [R_p]-$\mathbf{T_5XT_3/A_8}$; (—-) before UV irradiation, and (----) after irradiation.

The spectra of PS-modified A_5XA_3/T_8 ([R_p] isomer) and $\mathbf{T_5XT_3/A_8}$ ([R_p] isomer) duplexes in Figure 4b and c, respectively, show more or less similar CD pattern in the 250–280 nm region. This suggests that the global conformation of the PS-modified duplex is relatively insensitive to the stereochemistry of the PS-oligo backbone.

However, the CD spectra of the modified PS-oligos differed significantly from that of the native duplex (Fig. 4). They are marked by disappearance (in the spectrum of the latter) of a positive band at around 250 nm and a negative band around 277 nm, with appearance (in the spectrum of the former), respectively, of a negative band at 250 nm and a positive band at 280 nm, reflective of the influence on the modification on either of the strands.[18b]

The CD spectra of A_8X/T_8 and $\mathbf{T_8X/A_8}$ duplexes, in Figure 5a and b, respectively, reveal no significant change in the pattern (albeit, the spectra are marked by change in intensity), upon UV irradiation suggesting that incorporation of azobenzene, at the 3′-end of modified strands of the above duplexes, exerts little influence on the global conformation of the duplexes.

Prior to photomodulation, the CD spectrum of *E*-isomer of $\mathbf{T_7XT/A_8}$ ([S_p]) duplex (Fig. 5c) displays a maximum at 280 nm and a minimum at 255 nm along with weakly induced bands around 340–360 nm (π–π^* transition of the *E*-isomer). When the duplex is exposed to UV light, weak differences in the intensity of the CD bands are observed, albeit, the spectra exhibit overall similarity: a positive signal at 280 nm and a negative band centered at 255 nm. These spectral features perhaps reflect intercalation involving azobenzene and chirally stacked DNA base pairs.[27]

3. Conclusion

An efficient and simple strategy to tether an azobenzene moiety to oligonucleotides has been designed. The protocol provides flexibility concerning incorporation of azobenzene moiety at pre-selected sites in PS-oligomer sequences. Using the azobenzene-linked PS-oligonucleotides, modulation of the duplex was realized under UV–vis light. Owing to special importance of PS-oligos in antigene and antisense technology, the present investigations provide a potential methodology for affecting photomodulations in-vitro and in-vivo studies.

4. Experimental

4.1. *N*-Iodoacetyl-*p*-aminoazobenzene 1

To a pre-cooled solution of iodoacetic acid (576 mg, 3.1 mmol), dissolved in anhydrous THF (15 ml), was added *p*-aminoazobenzene (610 mg 3.1 mmol) followed by dropwise addition of a solution of DCC (640 mg, 3.1 mmol), dissolved in THF (10 ml), with constant stirring over a period of 15 min. The mixture was allowed to stir at 0 °C for 1 h followed by another 3 h at rt.

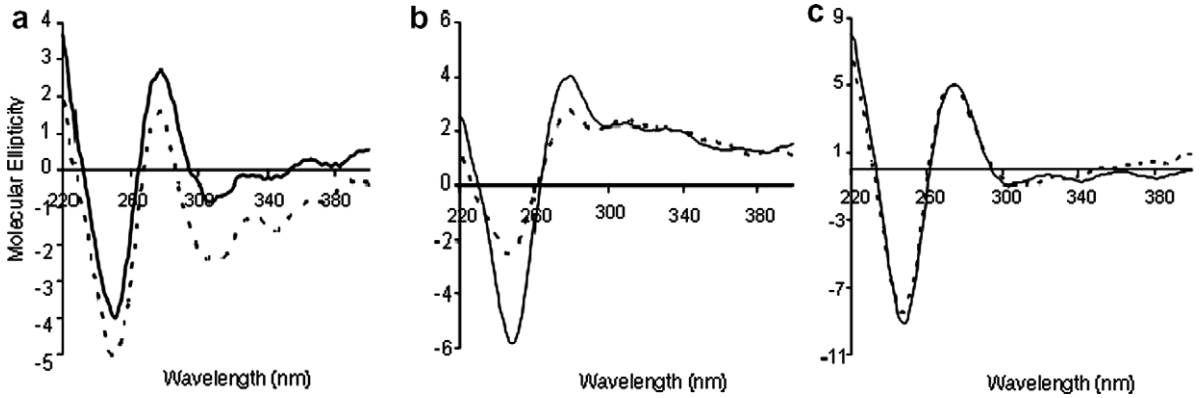

Figure 5. CD spectra of (a) duplex (A_8X/T_8), (b) $\mathbf{T_8X/A_8}$, (c) [S_p]-$\mathbf{T_7XT/A_8}$; (—-) before UV irradiation, and (----) after UV irradiation.

The reaction was monitored on TLC and the precipitated dicyclohexyl urea was removed by filtration. The filtrate was evaporated to dryness under vacuum and purified by silica gel chromatography. The compound was eluted with EDC and fractions containing the desired compound pooled together and concentrated to obtain **1** in 80% yield as a yellowish orange flaky material (903 mg). ^{1}H NMR ($CDCl_3$) δ: 7.83–7.93 (m, 4H, Ar-H), 7.46–7.53 (q, 3H, Ar-H), 7.67–7.69 (d, 2H, Ar-H), 3.89 (s, 2H, –CH_2–), 7.96 (s, 1H, –NHCO–). ESI-MS calculated for $C_{14}H_{12}N_3OI$ (M): 365.0. Found: 365.18. Mp: 172 °C. IR bands (thin film), ν cm^{-1} = (1100–1400), (1423–1440), 1498, 1538, 1605, 1636, (2923–3284). Elemental Anal. Calcd (%) for $C_{14}H_{12}N_3OI$: C, 46.05; H, 3.31; N, 11.51. Found: C, 45.93; H, 3.41; N, 11.39.

4.2. Preparation of polymer support for 3′-thiophosphated oligonucleotides

4.2.1. Mono 2-(4,4′-dimethoxytrityloxyethanesulfonyl)-ethyl succinate. A mixture of 2-(4,4′-dimethoxytrityloxyethylsulfonyl)-ethanol (456 mg, 1.0 mmol),[30] succinic anhydride (200 mg, 2.0 mmol), dry TEA (165 μl, 1.2 mmol), and DMAP (61 mg, 0.5 mmol) was dissolved in dry EDC (4 ml) and stirred for 30 min at rt. The reaction was monitored on TLC and quenched by addition of MeOH (0.5 ml). The reaction mixture was further diluted with EDC (20 ml) and washed successively with cold 5% aqueous citric acid (2× 15 ml) and saturated solution of NaCl (2× 15 ml). The organic phase was collected, dried over anhydrous Na_2SO_4, and concentrated to obtain the title compound (540 mg; 97% yield).

4.2.2. Attachment of the above succinate to 3-aminopropylated CPG. Mono 2-(4,4′-dimethoxytrityloxyethanesulfonyl)-ethyl succinate (28 mg, 50 μmol) was dissolved in MeCN (1.0 ml) and to this were added bromotrichloromethane (5 μl, 50 μmol) and DMAP (12.2 mg, 100 μmol). To the above, triphenylphosphine (6.55 mg, 25 μmol), dissolved in MeCN (0.5 ml), was added and the mixture was swirled for 30 s followed by addition of 3-aminopropylated CPG (250 mg).[31] The suspension was stirred for 30 min at rt. The support was recovered on a sintered glass funnel, washed with MeCN (5× 10 ml) and diethyl ether (2× 5 ml), respectively. This was dried under vacuum and subjected to capping (residual amino groups) with a solution consisting of Ac_2O/TEA/*N*-methylimidazole/DCM 1:1:0.4:6, v/v/v/v), for 30 min at rt. The functionalized polymer support was then washed, dried, and stored at 4 °C until used for oligonucleotide synthesis.

4.3. Oligonucleotide synthesis and purification

Modified and unmodified oligonucleotide sequences (Table 1) were synthesized at 0.2 μmol scale on a Pharmacia Gene Assembler Plus using the standard phosphoramidite approach following the manufacturer's protocol.[32] The phosphorothioate (PS)-linkage was incorporated at pre-selected positions in the oligonucleotides during synthesis cycle in a manner analogous to that in the normal cycle except that the oxidation step was replaced by a sulfurization step using (TETD) (0.5 M in MeCN)[33] in the machine. For introduction of thiophosphate at 3′-end, the oligomer was assembled on the modified polymer support **A** (Scheme 2). The cleavage of modified oligonucleotides from the solid support and simultaneous removal of protecting groups from internucleotide phosphates and exocyclic amino groups of nucleobases were achieved by treatment with aqueous NH_4OH (~30%) at 55 °C for 16 h. After deprotection, the ammoniacal solution was concentrated in speed vac, the residue dissolved in water (200 μl) and applied onto a desalting column (RP C-18 Silica Gel column). The oligomer was eluted with 30% MeCN in water, concentrated in a speed vac, and purified by anion exchange chromatography (FPLC). The configurational assignment of diastereomers, [R_p] and [S_p], and their separation from the stereo-mixture sequences were achieved by RP-HPLC.[19,20] The mass profiles of modified oligonucleotides were recorded on a Hewlett-Packard 1100 MSD Electron Spray Mass Spectrophotometer in the linear negative mode, which have been tabulated in Table 1.

4.4. Incorporation of azobenzene pendant into oligonucleotides

A stock solution of 2.73 mM concentration was prepared by dissolving **1** (1 mg) in DMF (1.0 ml). For coupling the azo derivative, **1**, with each of the modified phosphorothioate oligonucleotides, a pre-calculated amount of the oligomer was taken and 50-fold excess of the azo derivative was added to it. In a typical reaction, PS-4 (0.21 OD A_{254}) was dissolved in phosphate buffer (50 μl, pH 8.0). To this was added a solution of **1** (50 μl). The reaction mixture was then left on a shaker overnight. The solvent was removed in a speed vac, the residue dissolved in water (100 μl) and applied onto a Sephadex G-25 desalting column. The oligomer conjugate was eluted with 50.0 mM triethylammonium formate buffer, pH 7.1, and concentrated in a speed vac. Subsequently, the oligomer was subjected to purification by RP-HPLC. In a standard experiment, the elution pattern of [R_p] and [S_p] diastereomers of PS-4 phosphorothioate oligomer is shown in Figure 1a and b, where-as Fig. 1c and d depicts a co-injection of [R_p] and [S_p] diastereomers of PS-4 oligomer and azobenzene linked [R_p] diastereomer PS-4 oligomer, respectively. HPLC Conditions: Column, RP-18 Hypersil Gold; Gradient, 0–20% B in 15 min, A = 0.1 M $HCOONH_4$ buffer, pH 7.1, B = MeCN; flow rate, 1.0 ml/min.

Other PS-oligos conjugates were prepared and purified similarly.

4.5. Photomodulation of azobenzene-linked PS-oligonucleotides

Photomodulation of azobenzene conjugated modified PS-oligos was monitored using UV spectroscopy and RP-HPLC. In a typical experiment, the diastereomers, [R_p] and [S_p], of modified PS-oligo (PS-1) were separated by RP-HPLC. The attachment of azobenzene residue to

[S_p] diastereomer thus obtained, and its subsequent purification were achieved as described above. The azobenzene-tethered oligomer (0.5 OD A_{254nm}) was dissolved in distilled water and λ_{max} of *E*- and *Z*-isomers at 343 and 434 nm, respectively, were determined to calculate the molar extinction coefficients. Prior to irradiation, the molar extinction coefficient (ε) value for the *E*-isomer was found to be 2.4×10^4 cm^{-1} M^{-1} (at 343 nm), which accounted for ~91.6% of *E*-isomer and 8.4% of *Z*-isomer (at 434 nm). Subsequently, the stoppered optical cell was placed inside a photoreactor and irradiated for 30 min. Upon irradiation with UV light (365 nm), the value of *E*-isomer decreased to 1.14×10^4 cm^{-1} M^{-1} (82.3%) with concurrent increase in the *Z*-isomer (17.7%) indicating *E*–*Z* isomerization. The photostationary state, in this reaction, was achieved within 30 min (prolonged exposure of the sample did not display any further change in the spectral pattern). On exposure of the above sample (photostationary state) to visible light ($\lambda > 400$ nm), the value of ε for *E*-isomer increased to 1.82×10^4 cm^{-1} M^{-1} (corresponding to 89% *E*-isomer), showing reversible *E*–*Z* isomerization.

4.6. Thermal denaturation measurements

The thermal denaturation studies on the duplexes (Tables 2 and 3) were carried out on a UV–vis spectrophotometer. Two complementary strands were mixed together in equimolar concentration and subjected to heat treatment. All oligonucleotide sequences were hybridized to their complementary strands in 10 mmol phosphate buffer (pH 7.0) containing 1.0 M NaCl to obtain a concentration of 2 μM of each strand. In the case of *E*-isomers, the samples were heated for 20 min at 60 °C and then slowly cooled to 4 °C prior to denaturation studies. The same samples were irradiated at 365 nm for obtaining the *Z*-isomers, which were not subjected to the heat treatment and were kept at 4 °C as such prior to denaturation studies. Thermal denaturation profiles were recorded at 260 nm. Samples were equilibrated at 10 °C for 5–10 min prior to data collection. A heat-cool cycle in the temperature range of 10°–50 °C was supplied with a ramp of 0.5 °C/min with both *E*- and *Z*-isomers. In the case of *Z*-isomers, the samples were irradiated (365 nm) again prior to the next data acquisition. The melting temperature (T_m) of the duplexes was measured from the first derivative plots obtained from the thermal melting curves. Each experiment was repeated at least twice and the average was taken for T_m determinations. The reproducibility of the T_m values was within ±0.5 °C. A 1 ml volume capacity cell having 1 cm path length was used for the above denaturation studies.

4.7. Circular Dichroism measurements

The oligonucleotide sample solutions used for UV thermal melting studies were also used for CD experiments. Circular Dichroism studies of the samples were performed at 10 °C on a JASCO model J-715 spectropolarimeter equipped with a JASCO PTC-348WI Peltier temperature programmer. Optical cells with a path length of 1.0 cm were used. Absorbance values were taken over a range of 220–400 nm, at ~10 °C below the melting temperatures of all the duplexes. At least three runs were performed for recording the CD spectrum of each of the PS-modified duplexes. The final spectrum in each case was obtained after baseline subtraction and normalization of the respected CD curves.

Acknowledgment

Authors gratefully acknowledge financial support from the Department of Biotechnology, New Delhi, India.

References and notes

1. Dugave, C.; Demange, L. *Chem. Rev.* **2002**, *103*, 2475–2532.
2. Willner, I. *Acc. Chem. Res.* **1997**, *30*, 347–356.
3. Tamai, N.; Miyasaka, H. *Chem. Rev.* **2000**, *100*, 1875–1890.
4. Zhang, G.; Niu, A.; Peng, S.; Jiang, M.; Tu, Y.; Li, M.; Wu, C. *Acc. Chem. Res.* **2001**, *100*, 249–256.
5. Suginome, H. In *Handbook of Organic Photochemistry and Photobiology*; Horspool, W. M., Song, P.-S., Eds.; CRC Press: Boca Raton, FL, USA, 1995; p 824.
6. Yamana, K.; Yoshikawa, A.; Nakano, H. *Tetrahedron Lett.* **1996**, *37*, 637–640.
7. Yamana, K.; Kan, K.; Nakano, H. *Bioorg. Med. Chem.* **1999**, *7*, 2977–2983.
8. Asanuma, H.; Ito, T.; Komiyama, M. *Tetrahedron Lett.* **1998**, *39*, 9015–9018.
9. Asanuma, H.; Yoshida, T.; Ito, T.; Komiyama, M. *Tetrahedron Lett.* **1999**, *40*, 7995–7998.
10. Yamazawa, A.; Liang, X.; Asanuma, H.; Komiyama, M. *Angew. Chem. Int. Ed.* **2000**, *39*, 2356–2357.
11. Asanuma, H.; Tamaru, D.; Yamazawa, A.; Liu, M.; Komiyama, M. *ChemBioChem* **2002**, *3*, 786–789.
12. Asanuma, H.; Liang, X.; Yoshida, T.; Komiyama, M. *Angew. Chem. Int. Ed. Engl.* **2000**, *39*, 1316–1318.
13. Liang, X. G.; Asanuma, H.; Komiyama, M. *J. Am. Chem. Soc.* **2002**, *124*, 1877–1883.
14. Liang, X. G.; Asanuma, H.; Komiyama, M. *Tetrahedron Lett.* **2001**, *42*, 6723–6725.
15. Asanuma, H.; Takarada, T.; Yoshida, T.; Tamaru, D.; Liang, X.; Komiyama, M. *Angew. Chem. Int. Ed.* **2001**, *40*, 2671–2673.
16. Asanuma, H.; Ito, T.; Yoshida, T.; Liang, X.; Komiyama, M. *Angew. Chem. Int. Ed.* **1999**, *38*, 2393–2395.
17. Matsunaga, D.; Asanuma, H.; Komiyama, M. *J. Am. Chem. Soc.* **2004**, *126*, 11452–11453.
18. (a) Asanuma, H.; Liang, X.; Komiyama, M. *Tetrahedron Lett.* **2000**, *41*, 1055–1058; (b) Asanuma, H.; Liang, X. G.; Yoshida, T.; Komiyama, M. *ChemBioChem* **2001**, *2*, 39–44.
19. Tamura, Y.; Miyoshi, H.; Yokota, T.; Makino, K.; Mukami, A. *Nucleosides Nucleotides* **1998**, *17*, 269–282.
20. Saenger, W. In *Principles of Nucleic Acid Structure*; Springer: New York, 1984.
21. Suggs, J. W.; Taylor, D. A. *Nucleic Acids Res.* **1985**, *13*, 5707–5716.
22. Cosstick, R.; Eckstein, F. *Biochemistry* **1985**, *24*, 3630–3638.
23. Robertson, J. M. *J. Chem. Soc.* **1939**, 232–236.
24. Letsinger, R. L.; Schott, M. E. *J. Am. Chem. Soc.* **1981**, *103*, 7394–7396.

25. Fukuda, R.; Takenaka, S.; Takagi, M. *J. Chem. Soc. Chem. Commun.* **1990**, 1028–1030.
26. Kubota, M.; Ono, A. *Tetrahedron Lett.* **2004**, *45*, 1187–1190.
27. Lyng, R.; Hard, T.; Norden, B. *Biopolymers* **1987**, *26*, 1327–1345.
28. Clark, C. L.; Cecil, P. K.; Singh, D.; Gray, D. M. *Nucleic Acids Res.* **1997**, *25*, 4098–4105.
29. Shimazu, M.; Shinozuka, K.; Sawai, H. *J. Chem. Soc., Perkin Trans. 1* **2002**, 1778–1785.
30. Urdea, M. S.; Horn, T. *Tetrahedron Lett.* **1986**, *27*, 2933–2936.
31. Fritz, J. S.; King, J. N. *Anal. Chem.* **1976**, *48*, 570–572.
32. Pharmacia. LKB Gene Assembler Plus Manual, Upsala, Sweden.
33. Vu, H.; Hirschbein, B. L. *Tetrahedron Lett.* **1991**, *32*, 3005–3008.